Egyptian Journal of Aquatic Biology & Fisheries
Zoology Department, Faculty of Science,
Ain Shams University, Cairo, Egypt.
ISSN 1110 – 6131
Vol. 27(2): 645 – 659 (2023)
www.ejabf.journals.ekb.eg

Algae-Mediated Synthesis and Structural Characterization of Silver Nanoparticles from *Laurencia papillosa* and *Galaxaura rugosa*

Ahlam S. El Shehawy[1], Ashraf Elsayed[1], Omar A. El-Shehaby[1], Elham M. Ali[2,3,*]

[1] Department of Botany, Faculty of Sciences, University of Mansoura, Egypt
[2] Department of Environmental Studies, The National Authority for Remote Sensing and Space Sciences
[3]Depatrment of Aquatic Environment, Faculty of Fish Resources, University of Suez, Egypt

***Corresponding Author: elhamali201212@yahoo.co.uk - elhamali@narss.sci.eg**

ARTICLE INFO
Article History:
Received: March 18, 2023
Accepted: April 9, 2023
Online: April 27, 2023

Keywords:
Algae,
Laurencia papillosa,
Galaxaura rugosa,
Biosynthesis,
Ag nanoparticles,
Characterization

ABSTRACT

Laurencia papillosa and *Galaxaura rugosa-mediated* silver nanoparticles (AgNPs) were successfully synthesized by a simple reduction method. The AgNPs were characterized using UV–visible spectroscopy, X-ray diffraction analysis (XRD), transmission electron microscopy (TEM), Selected area electron diffraction (SAED), scanning electron microscopy (SEM), energy dispersive analysis of X-rays (EDAX), zeta potential and fourier transform infrared spectroscopy (FTIR). Rapid color change from yellow to dark brown and UV-visible absorption peaks for *L. papillosa* at 398 and 458 nm and *G. rugosa* at 409 nm, respectively, supported the early formation of AgNPs. Biogenic AgNPs were face-centered cubic, crystalline and spherical, with mean diameter sizes varying from 6.9 to 15.0 nm for *L. papillosa* and 5.8 to 13.8 nm for *G. rugosa*, according to XRD, TEM and SAED analyses. The high abundance of AgNPs produced by *L. papillosa* and *G. rugosa* was visible in SEM, and the particles almost resembled spheres and in aggregates. For *L. papillosa* and *G. rugosa*, the biosynthesized AgNPs had a negative surface charge with zeta potential values of -17.8 mV and -16.4 mV, respectively. According to FTIR findings, functional groups significantly contribute to the bioreduction of silver ions and the stability of AgNPs. This approach is simple and safe for the environment, and it can be used for projects with a focus on the environment.

INTRODUCTION

Nanoparticles (NPs) are very small particles with dimensions ranging from 1–100 nm in size **(Elumalai *et al.*, 2010)**. Due to their small dimensions, they have several unique characterizations, such as high electrical properties, mechanical and thermal stability, surface area, and optical and magnetic properties **(Yaqoob *et al.*, 2020b)**. The enhanced properties of nanomaterials have qualified them for use in different fields, such as wastewater treatment, drug delivery, different medical and biological tools, chemical

and biological sensors and electronic devices industries **(Bolaños-Guerrón *et al.*, 2023; Dubadi *et al.*, 2023; Luo, 2023; Unnisa *et al.*, 2023)**.

Noble metal nanoparticles have attracted significant interest in the scientific community due to their specific photothermal and optical properties **(Yaqoob *et al.*, 2020a)**, of which silver nanoparticles (AgNPs) got much interest due to their chemical stability, good conductivity, catalytic function, as well as being good antimicrobial agents (antibacterial, antiviral, and antifungal), in addition to their anti-inflammatory activities, which allow them to incorporate into different textile industries, cryogenic superconducting materials, cosmetic products, food industry and manufacturing of electronic components **(Paulraj *et al.*, 2020; González-Pedroza *et al.*, 2023)**.

In general, NPs have been fabricated by several well-established physical and chemical methods **(Rane *et al.*, 2018)**, which are known to be costly, involving complex facilities, hazardous flammable chemicals and high temperatures **(Ramya & Subapriya, 2012)**. Therefore, researchers have recently focused on employing biological-based approaches for nanoparticles synthesis since they are generally cost-effective, nontoxic, scalable and eco-friendly **(Thakkar *et al.*, 2010)**. In the last few decades, bacteria **(Anil *et al.*, 2023)**, several plant extracts **(Dangana *et al.*, 2023)**, enzymes **(Loi *et al.*, 2023)**, fungi **(Soliman *et al.*, 2023)** and algae **(Palaniyandi *et al.*, 2023)** have already been used for the synthesis of NPs. Among those biological sources, algae are known as the 'bionanofactories' because their life and dead dried biomasses could be used to synthesize metallic nanoparticles **(Davis *et al.*, 1998)**. Therefore, algae are extensively explored as a potential tool for green synthesis of metallic nanoparticles based on their high capacity for metal accumulation, the convieniance of culture and ease handle, the low need for energy (i.e. temperature) with greater efficiency, the less toxicity and risk to the environment **(Sharma *et al.*, 2016)**. Marine algal seaweeds, in particular, could produce nanoparticles quite stable in solution as various biomolecules, including polysaccharides, peptides and pigments responsible for metals reduction, stability and capping of the metal nanoparticles **(Singaravelu *et al.*, 2007)**.

Based on the aforementioned information, the present study was designed aiming at studying the potential application of marine red algae for green biosynthesis of AgNPs, using two different macroalgal species; namely, *L. papillosa* and *G. rugosa*. In addition, different characterization processes were used for better identification of the biosynthesized nanomaterials of AgNPs.

MATERIALS AND METHODS

Chemicals used in the study

All the reagents and chemicals employed in this study were acquired from Sigma, Egypt, and they have scientific grade. Freshly prepared double-distilled water was used throughout the experimental work.

Algal sampling and preparation of algal extract

L. papillosa and *G. rugosa* were collected by hand from littoral zone in June 2021 from Zaafran beach **(**latitudes 29.06" N and longitudes 32.43" E) located in the Suez Gulf, the Red Sea, Egypt; it is 82 km south of Alain AL Sokhna (see fig. 1). Seaweeds samples were carried in seawater using plastic bags to prevent evaporation until reaching the laboratory within 2-3 hours of collection. The epiphytic and extraneous matter was removed by several washes with seawater, followed by fresh tap water, followed by distilled water and then left to dry in a shadow place for about two weeks. The dried algal materials were crushed using liquid nitrogen to be in a powder form and stored in an air-tight container at 4°C until use. About 5g of each crushed algal powder was added to 100 ml of deionized water in a 250ml conical flask, soaking for 24 hours with shaking. Both extracts were filtered through Whatman No 1 filter paper, of which the supernatants were used for the preparation of AgNPs **(Kumar *et al.*, 2013)**.

Fig. 1. Map showing the collection site of the used seaweeds in Zaafrana beach, Red Sea, Egypt

AgNPs synthesis

The established protocol reported by **Fatima *et al.* (2020)** was applied to synthesize silver nanoparticles. 45ml of silver nitrate solution was procured with 1 mM concentration and supplemented slowly with 5ml of each algal extract with continuous stirring at room temperature. On incubation for 24h, the color changes into dark brown representing the formation of nanoparticles. After a proper reduction reaction, the solution was centrifuged at 14,000 rpm for 5min. The product was then washed several times with acetone and then dried for 24h to obtain the purified AgNPs. The dried nanoparticles were ground and stored at 7℃ for the characterization process.

Characterization of silver nanoparticles

UV–visible spectroscopy. The formation of Ag NPs was analyzed with the UV–visible spectroscope (Uni cam UV-VIS. Spectrometer UV2, U.S.A). The reaction mixtures were subjected to varied wavelengths ranging from 400 to 500 nm, and the peak was studied to regulate the wavelengths at which nanoparticles got synthesized.

XRD. It was obtained by a DX-1000 X-ray powder diffractometer operated at 40 kV and 30 mA, in the 2θ range of 10°–90°.

TEM. The average size and the intrastructures of the nano-colloidal sample were visualized by TEM JEOLJEM-2100, U.S.A, using a carbon-coated grid (Type G 200, 3.05μ diameter, TAAP, U.S.A).

SAED. It is a crystallographic experimental technique that can be performed inside a transmission electron microscope. It is used for the analysis of crystalline structure, crystalline defect, and crystalline lattice parameters.

SEM. The FEI-TITAN 80–300 kV SEM was used to study the AgNPs elemental, morphological, and size.

EDAX. The elements presented in NPs were determined by EDAX integrated into a scanning electron microscope to confirm the AgNPs occupancy in the sample and to detect any other elementary compositions.

Zeta potential

The nano-colloidal solution stability and surface charge of nanoparticles are measured by Photon Correlation Spectroscopy (PCS) (Malvern Zeta size Nano-zs90, U.S.A).

FTIR. The powder of both algal species and AgNPs was recorded in the 400–4000 cm^{-1} range in a Shimadzu IRAfnity-1 spectrometer (Shimadzu, Japan) to determine the main components of algae extracts and determine the biomolecules involved in the synthesis of NPs.

RESULTS

1. Taxonomic description of seaweed samples

Before the synthesis application, both collected algae were identified and then classified. Species identification and taxonomical classification were done by a classification expert using fresh samples on the same collection day. Both species are red algae (Rhodophyta); namely, *Laurencia obtusa* var. *papillosa* (C.Agardh), family Rhodomelaceae (Fig.1a), and *Galaxaura rugosa* (J.Ellis & Solander), family Galaxauraceae (Fig.1b).

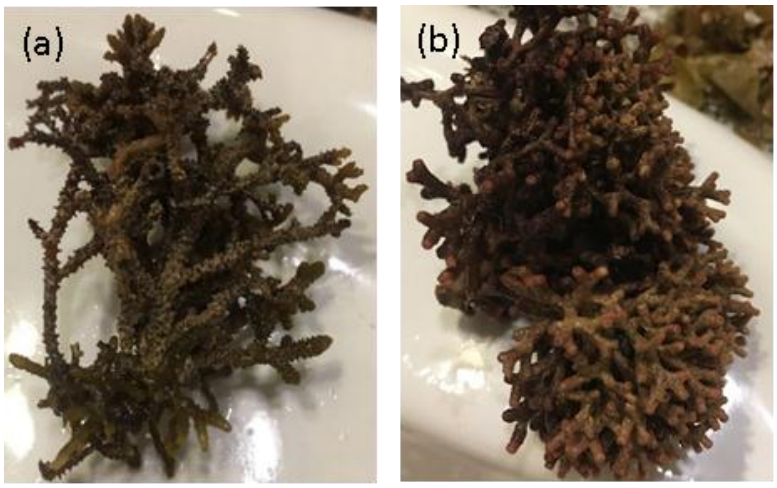

Fig. 2. Photos of the studied seaweeds showing: **(a)** *Laurencia obtusa* and **(b)** *Galaxaura rugosa.*

2. Biosynthesis of silver nanoparticles

The color transformation of the solution after adding the algal extracts to the AgNO3 solution is the preliminary indication for the formation of silver nanoparticles. Before adding the algae extracts to the $AgNO_3$ solution, it was colorless and on adding the algal extract the color appeared deep dark brown after incubation for 24h. It was transformed from yellowish brown in the case of *L. papillosa* extracts and from pale yellow in the case of *G. rugosa* (Fig. 3), indicating the production of AgNPs.

Fig. 3. Photo for the experiment showing the color change of both algal extracts; *L. papillosa* and *G. rugosa* on the addition of 10^{-3} M colorless solution of $AgNO_3$

3. Characterization of silver nanoparticles from seaweed extracts

3.1. UV-analysis

UV–visible spectroscopy was used with the wavelength range of 200–700 nm to confirm the synthesis of the algae-mediated silver nanoparticles. The maximum absorption peak for AgNPs from *L. papillosa* was observed at 398 nm and 458 nm while from *G. rugosa* it was observed at 409 nm (Fig. 4, represented as a star), characterizing

the AgNPs synthesis. The two algae extracts didn't show any characteristic peaks in the visible region.

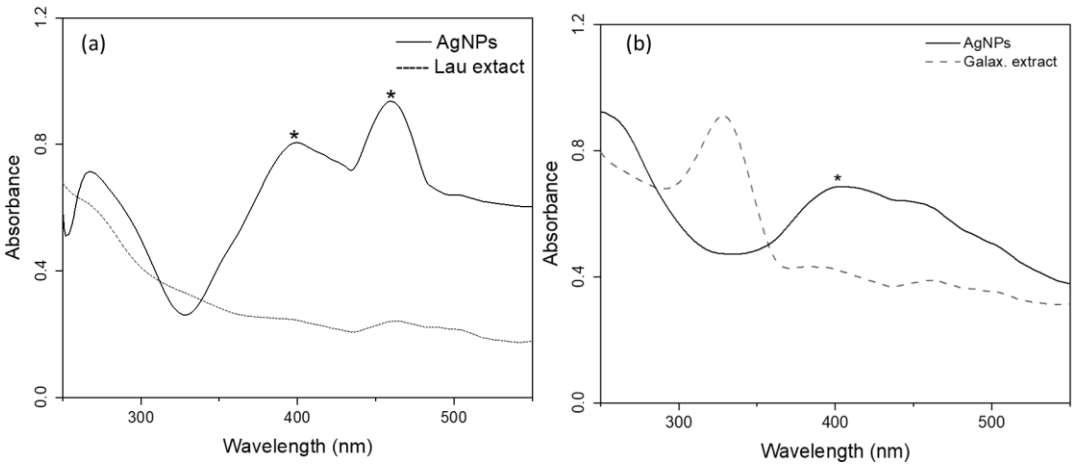

Fig. 4. UV–visible spectra of AgNPs biosynthesized from **(a)** *L. papillosa and* **(b)** *G. rugosa* extracts

3.2. XRD analysis

The XRD analysis was used to identify the phase and the nano-crystalline structure of the biosynthesized silver nanoparticles. Intense AgNPs diffraction peaks were clearly observed, as shown in Fig. (5). The major observed XRD peaks for *L. papillosa* and *G. rugosa* AgNPs were observed at 2θ values of 27.79°, 32.17°, 38.03°, 46.11°, 54.83° and 57.39°, which are indexed to (210), (122), (111), (200), (231), (142) and (241) planes. The distinct XRD reflection planes confirm the face-centered cubic (FCC) crystal morphology with the JCPDS Card No. 04-0783. Other peaks were observed by the diffractogram at 27.74°, 29.63°, 32.155° and 46.18°; this could be corresponded to the reducing and capping organic moieties attached to AgNPs.

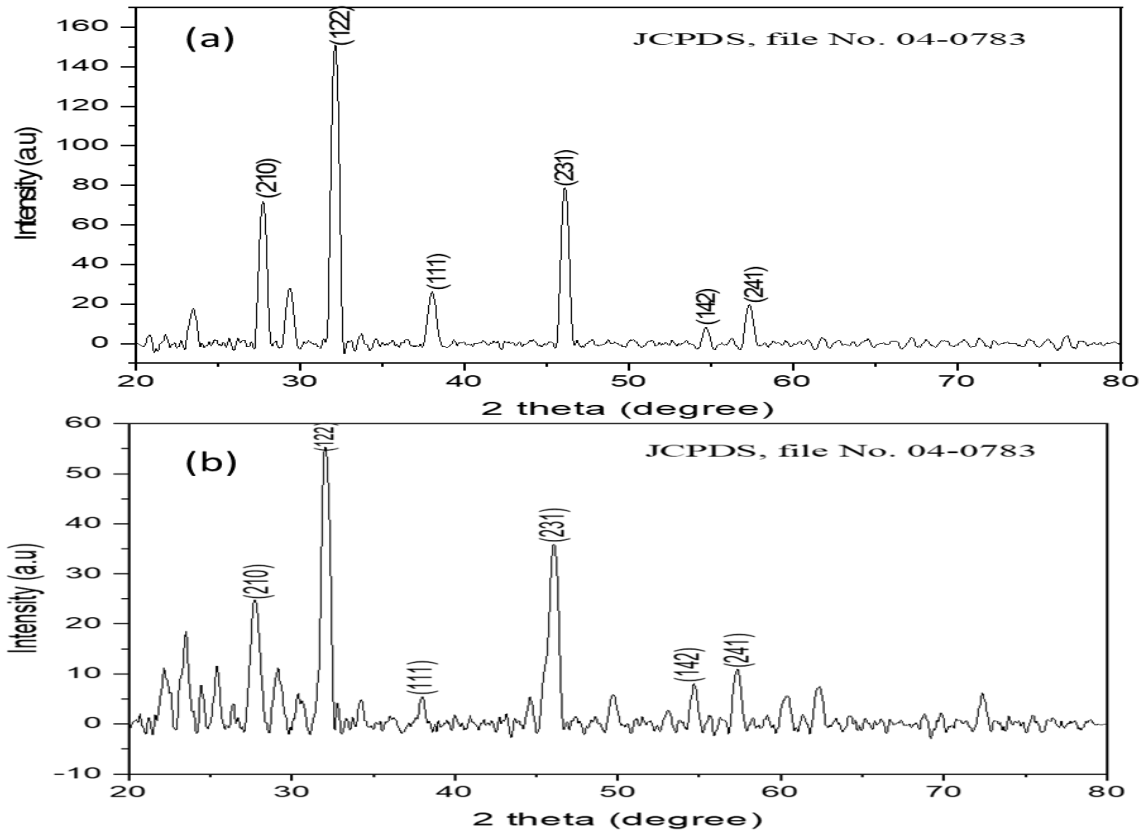

Fig. 5. X-ray diffractive peaks of AgNPs biosynthesized from **(a)** *L. papillosa* and **(b)** *G. rugosa* extracts

3.3. TEM analysis

Morphological features of the biologically obtained AgNPs were investigated using TEM that showed almost spherical structures (Fig. 6), with particles' average size ranging from 6.9 to 15.0 nm for *L. papillosa* and from 5.8 to 13.8 nm for *G. rugosa*.

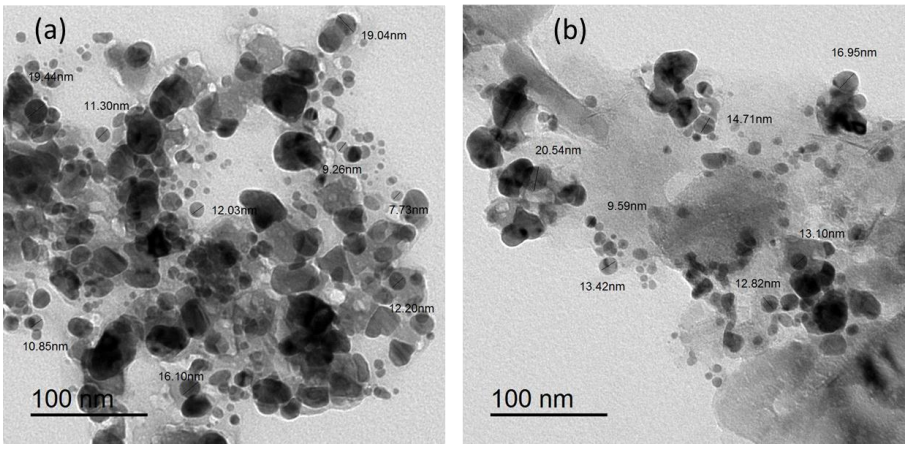

Fig. 6. TEM micrograph of AgNPs biosynthesized from **(a)** *L. papillosa* and **(b)** *G. rugosa* extracts

3.4. SEM analysis

The generated silver nanoparticles were further characterized by SEM to investigate the particle surface morphology. Results indicate that the surface of AgNPs was uniform, the high density of AgNPs is synthesized by *L. papillosa* and *G. rugosa*, the particles appeared are nearly spherical and are found to be in aggregates (Fig. 7).

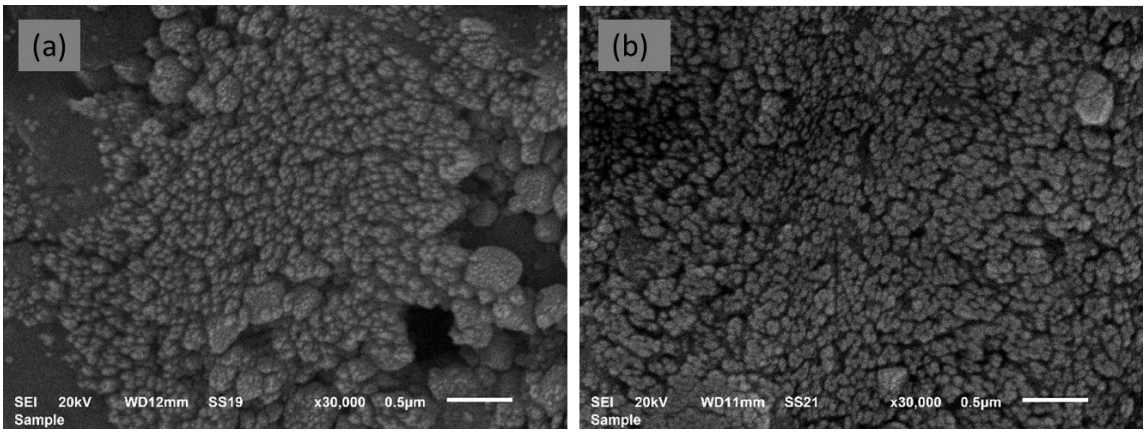

Fig. 7. SEM micrograph of AgNPs synthesized from **(a)** *L. papillosa* and **(b)** *G. rugosa* extracts

3.5. EDEX analysis

The EDEX analysis was carried out to define the elemental composition of the biosynthesized silver nanoparticles. A strongly distinctive EDX spectrum was observed at 3KeV which confirmed the synthesis of silver nanoparticles, as shown in Fig. (8). Some other peaks were observed for chlorine, carbon, oxygen, aluminum, calcium and silica (Fig. 8).

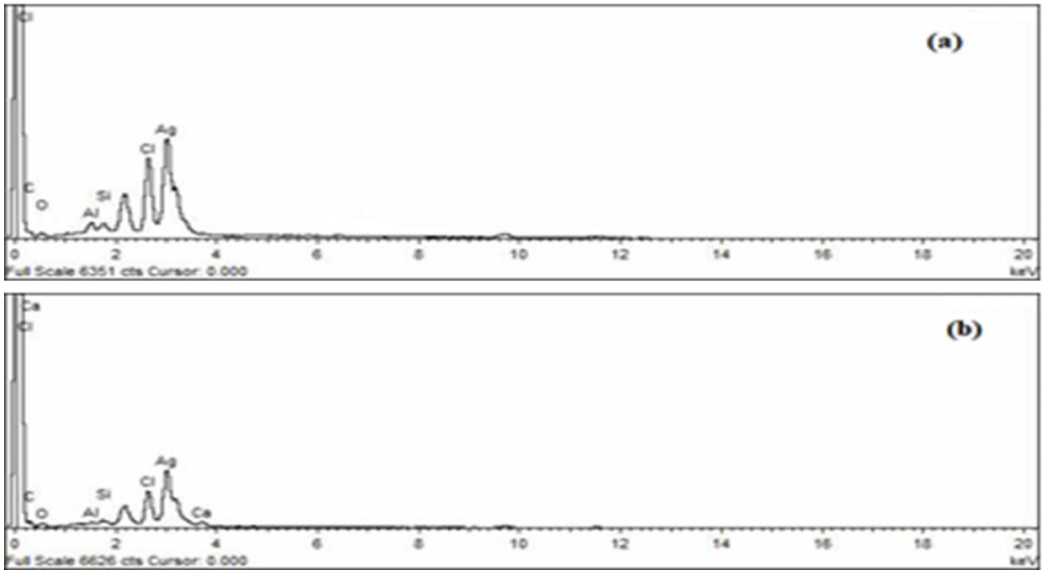

Fig. 8. EDX spectra of AgNPs biosynthesized from **(a)** *L. papillosa* and **(b)** *G. rugosa* extracts

3.6. Zeta potential analysis

The stability of nanoparticles in aqueous solutions can be tested by the zeta potential; the measure of surface charge potential. AgNPs' zeta potential measurements showed that *L. papillosa* and *G. rugosa* got negative mean zeta potentials of -17.8 mV and -16.4 mV, respectively (Fig. 9).

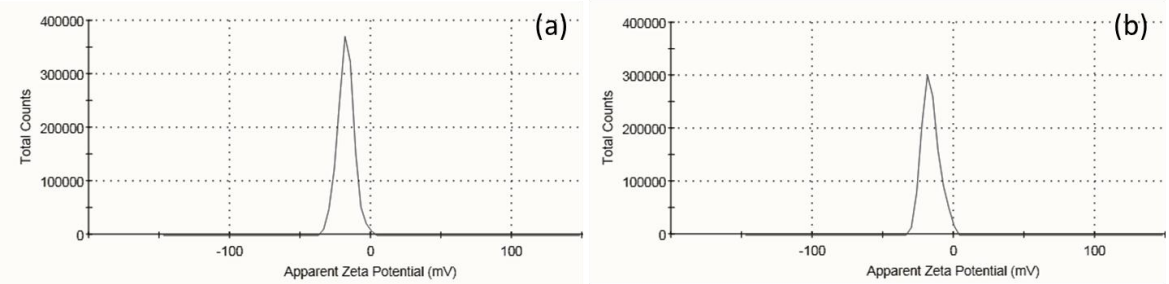

Fig. 9. Zeta potential of AgNPs biosynthesized from **(a)** *L. papillosa* and **(b)** *G. rugosa* extracts

3.7. FTIR analysis

FTIR assessment was carried out for AgNPs, *L. papillosa* extract and *G. rugosa* extracts to study the possible working classes interacting with silver and algae combination. As shown in Fig. (10), major peaks appeared at 3421, 1598, 1384, 1035, and 865 cm^{-1}, in correspondence to the stretching of the N-H bond in amines, and O-H in alcohols, C = C bond stretching in alkene, N-O bond stretching in the nitro compound, O-H bond stretching in carboxylic acid, and C = C bond bending in alkenes, respectively. *L. papillosa* and *G. rugosa* extracts and AgNPs reflect a similar overall pattern with variations in their strength.

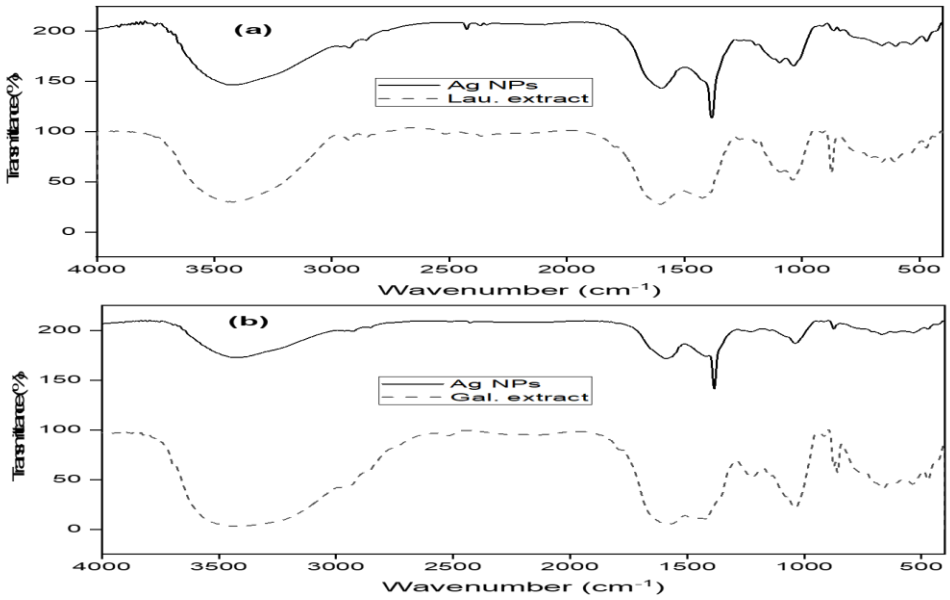

Fig. 10. Results of the FTIR assessment for extracts of **(a)** *L. papillosa*, **(b)** *G. rugosa* and their corresponding AgNPs

DISCUSSION

A green technology approach has been employed in this research to biologically synthesize nanoparticles, coinciding with the global interest of most research communities. This is attributed to several factors, mainly including simplicity of application, nontoxicity action, and less time and cost requirements. One of the major reasons to transform to the green synthesis of NPs is the feasibility of large-scale manufacturing **(Al-Radadi *et al.*, 2022)**, which is increasing the concern about this approach worldwide. The current study successed to generate AgNPs biologically using algal extracts of two red algae, *L. papillosa* and *G. rugosa*. Generation confirmation, identification and characterization of the delivered nanoparticles (AgNPs) were conducted through several different standard analytical techniques, including UV–visible spectroscopy, XRD, SEM, EDAX and FTIR.

The primary indication of successful biosynthesis of AgNPs is the change in the color of the solutions, which displays a brown color **(Fatima *et al.*, 2020)**. Surface plasmon resonance (SPR), which was the result of the minimising action, was responsible for the change in the solution's appearance **(Shantkriti *et al.*, 2023)**.

UV-Vis spectrophotometry is the main technique for elucidating the formation of AgNPs during the earliest phases of synthesis **(Paramelle *et al.*, 2014)**. The biosynthesized AgNPs showed peaks at 398 nm and 458 nm for *L. papillosa* and 409 nm for *G. rugosa*. These nanoparticles are thought to be significantly absorbed in the UV-vis range due to the SPR caused by the obvious interaction between the incoming light and electrons present in the conduction band on the AgNPs surface **(Singaravelan & Bangaru Sudarsan Alwar, 2015)**. This result is in agreement with previous studies **(Loi *et al.*, 2023; Soliman *et al.*, 2023)**. The presence of dual or additional bands in *L. papillosa* indicates the synthesis of nanoparticles of various sizes and shapes **(Cepoi *et al.*, 2015)**, while a single SPR band in *G. rugosa* indicates the formation of spherical nanoparticles **(Somasundaram *et al.*, 2021)**.

The XRD technique is an exceptional methodology for supporting the fabrication of nanoparticles because it delivers information about structural configurations. XRD spectrum was compared with the International Center of Diffraction Data card (JCPDS, file No. 04-0783) and showed the diffraction peaks of the Ag nanocrystals as evident from the peaks correspondence to 210, 122, 111, 200, 231, 142 and 241planes, which have been indexed for silver **(Fatima *et al.*, 2020)**. The XRD results clearly show a number of Braggs reflections that confirm the FCC crystalline nature of AgNPs, which is in accordance with the results reported by other similar studies **(Zahran & Mohammed, 2021)**. Other unidentified peaks in the X-ray diffraction pattern with relatively lower intensities may be the result of extract-derived inorganic or organic components crystallizing on the surface of AgNPs **(Rezazadeh *et al.*, 2020)**.

The crystalline nature of synthesized silver nanoparticles as confirmed by TEM showed spherical structures for both *L. papillosa* and *G. rugosa* extracts (Fig. 4). These

results agree with previous results **(Algotiml *et al.*, 2022)**. The current findings depicted different AgNPs shapes compared to previously reported studies **(El-Kassas & El Komi, 2014)**. This outcome could be a result of the various algae species that were collected at sample locations in the Red Sea under various environmental circumstances. Additionally, the size of the nanoparticles in the present study was smaller than that in **(Faisal *et al.*, 2020)**, which may be related to the different methodologies, synthesis conditions (such as temperature and incubation time), handling procedures, and metabolites used for capping and reduction of silver ions (such as different metabolites).

The SEM images display the generated silver nanoparticles' spherical form, which is a characteristic of the particles generally. By utilising green algae, similar outcomes were also described in the study of **Al-Radadi *et al.* (2022)** by utilizing green algae. AgNPs' tendency to aggregate could be explained by the bioactive components in the preparations that form a layer on top of them **(Ghasemi *et al.*, 2023)**.

Signals from the EDAX analysis at 3 keV support the formation of silver nanoparticles **(Naghmouchi *et al.*, 2022)**. The same EDX pattern of AgNPs with high purity was recorded in the study of **Al-Radadi *et al.* (2022)**. However, extra peaks in the spectrum were observed, indicating that algae biomolecules were involved in the synthesis of nanoparticles **(Abdel-Raouf *et al.*, 2018)**. The presence of chlorine could be due to the purified water used to create the aqueous extract of the marine algae used as part of the synthesis medium for silver nanoparticles **(Bhuyar *et al.*, 2020)**. Reactive oxygen that has been adsorbed onto the surface of AgNPs could be the source of a weak O signal **(Rezazadeh *et al.*, 2020)**.

Using zeta potential readings, the stability of the nanoparticles was evaluated (-17.8 mV and -16.4 mV for *L. papillosa* and *G. rugosa*, respectively). The negative potential values could be due to the capping impact of the biomolecules present in the *L. papillosa* and *G. rugosa* algal extracts. Additionally, they showed the longevity of the nanoparticles by demonstrating how they repel one another, which prevents the accumulation of nanoparticles **(Patil *et al.*, 2012)**. The results are consistent with those obtained using silver nanoparticles made from Azadirachta indica **(Nagar & Devra, 2019)**.

CONCLUSION

Through this research we found that, the production of silver nanoparticles from seaweeds is a way that is both safer and more environmentally friendly than competing techniques. To conclude, producing silver nanoparticles is made easy by using the extracts of the red algae *L. papillosa* and *G. rugosa* as a capping and reducing agent. The two algae extracts stabilize the silver ions in the reduction process and prevent the oxidation of silver ions protecting them from outside effects, as shown by advanced spectroscopic analysis using UV-visible spectroscopy, XRD, SEM, EDAX and FTIR. These cutting-edge biogenic and eco-friendly technologies are suitable for use in a wide

range of sectors because the produced nanoparticles are quite stable for prolonged periods without significant alteration.

FUNDING SOURCES

This work was supported by Science, Technology & Innovation Funding Authority (STDF), Egypt [Post Graduate Support Grant (PGSG), Post Graduate Support, Non-Industrial sector, National, grant number 45049].

REFERENCES

Abdel-Raouf, N.; Alharbi, R.M.; Al-Enazi, N.M.; Alkhulaifi, M.M. and Ibraheem, I.B.M. (2018)**.** Rapid biosynthesis of silver nanoparticles using the marine red alga Laurencia catarinensis and their characterization. Beni-Suef University Journal of Basic and Applied Sciences, 7(1): 150-157.

Al-Radadi, N.S.; Hussain, T.; Faisal, S. and Shah, S.a.R. (2022)**.** Novel biosynthesis, characterization and bio-catalytic potential of green algae (Spirogyra hyalina) mediated silver nanomaterials. Saudi Journal of Biological Sciences, 29(1): 411-419.

Algotiml, R.; Gab-Alla, A.; Seoudi, R.; Abulreesh, H.H.; El-Readi, M.Z. and Elbanna, K. (2022)**.** Anticancer and antimicrobial activity of biosynthesized Red Sea marine algal silver nanoparticles. Scientific reports, 12(1): 1-18.

Anil, A.; Sanjeev, K.; Kamarudheen, N.; Sebastian, P.M. and Rao, K.B. (2023)**.** EPS-mediated biosynthesis of nanoparticles by Bacillus stratosphericus A07, their characterization and potential application in azo dye degradation. Archives of Microbiology, 205(2): 72.

Bahrami, F.; Yu, X.; Zou, Y.; Sun, Y. and Sun, G. (2020)**.** Impregnated calcium-alginate beads as floating reactors for the remediation of nitrate-contaminated groundwater. Chemical Engineering Journal, 382: 122774.

Bhuyar, P.; Rahim, M.H.A.; Sundararaju, S.; Ramaraj, R.; Maniam, G.P. and Govindan, N. (2020)**.** Synthesis of silver nanoparticles using marine macroalgae Padina sp. and its antibacterial activity towards pathogenic bacteria. Beni-Suef University Journal of Basic and Applied Sciences, 9(1): 1-15.

Bolaños-Guerrón, D.; Galarza, I.; Llumiquinga, E.; Toulkeridis, T. and Cumbal, L. (2023)**.** Design and Construction of a Prototype for Arsenic Retention in Mining-Contaminated Waters by Application of Nanoparticles-Based Technosols. Sustainability, 15(2): 1286.

Cepoi, L.; Rudi, L.; Chiriac, T.; Valuta, A.; Zinicovscaia, I.; Duca, G.; Kirkesali, E.; Frontasyeva, M.; Culicov, O. and Pavlov, S. (2015)**.** Biochemical changes in cyanobacteria during the synthesis of silver nanoparticles. Canadian journal of microbiology, 61(1): 13-21.

Dangana, R.S.; George, R.C. and Agboola, F.K. (2023)**.** The biosynthesis of zinc oxide nanoparticles using aqueous leaf extracts of Cnidoscolus aconitifolius and their biological activities. Green Chemistry Letters and Reviews, 16(1): 2169591.

Davis, S.A.; Patel, H.M.; Mayes, E.L.; Mendelson, N.H.; Franco, G. and Mann, S. (1998)**.** Brittle bacteria: a biomimetic approach to the formation of fibrous composite materials. Chemistry of Materials, 10(9): 2516-2524.

Dubadi, R.; Huang, S.D. and Jaroniec, M. (2023)**.** Mechanochemical Synthesis of Nanoparticles for Potential Antimicrobial Applications. Materials, 16(4): 1460.

El-Kassas, H.Y. and El Komi, M.M. (2014)**.** Biogenic silver nanoparticles using seaweed Ulva rigida and their fungicidal and cytotoxic effects. JKAU Mar Sci, 25: 3-20.

Elmayah, N.M.; El-Fallal, A.A.; Abou-Dobara, M.I. and Khalifa, M.E. (2022)**.** Response Surface Method for Optimizing the Biosynthesis of Silver Nanoparticles Using Talaromyces stipitatus and Their Antimicrobial Activity. Jordan Journal of Biological Sciences, 15(3).

Elumalai, E.; Prasad, T.; Hemachandran, J.; Therasa, S.V.; Thirumalai, T. and David, E. (2010)**.** Extracellular synthesis of silver nanoparticles using leaves of Euphorbia hirta and their antibacterial activities. J Pharm Sci Res, 2(9): 549-554.

Faisal, S.; Shah, S.A.; Shah, S.; Akbar, M.T.; Jan, F.; Haq, I.; Baber, M.E.; Aman, K.; Zahir, F. and Bibi, F. (2020)**.** In vitro biomedical and photo-catalytic application of bio-inspired zingiber officinale mediated silver nanoparticles. Journal of Biomedical Nanotechnology, 16(4): 492-504.

Fatima, R.; Priya, M.; Indurthi, L.; Radhakrishnan, V. and Sudhakaran, R. (2020)**.** Biosynthesis of silver nanoparticles using red algae Portieria hornemannii and its antibacterial activity against fish pathogens. Microbial pathogenesis, 138: 103780.

Ghasemi, S.; Harighi, B. and Ashengroph, M. (2023)**.** Biosynthesis of silver nanoparticles using Pseudomonas canadensis, and its antivirulence effects against Pseudomonas tolaasii, mushroom brown blotch agent. Scientific reports, 13(1): 3668.

González-Pedroza, M.G.; Benítez, A.R.T.; Navarro-Marchal, S.A.; Martínez-Martínez, E.; Marchal, J.A.; Boulaiz, H. and Morales-Luckie, R.A. (2023)**.** Biogeneration of silver nanoparticles from Cuphea procumbens for biomedical and environmental applications. Scientific reports, 13(1): 790.

Kumar, P.; Senthamil Selvi, S. and Govindaraju, M. (2013)**.** Seaweed-mediated biosynthesis of silver nanoparticles using Gracilaria corticata for its antifungal activity against Candida spp. Applied Nanoscience, 3(6): 495-500.

Loi, H.R.; Abbasiliasi, S.; Raja, P.B.; Mohamed, M.S.; Tan, W.-N.; Ng, H.S.; Lan, J.C.-W. and Tan, J.S. (2023)**.** Biosynthesis of silver nanoparticles using nitrate reductase produced by Lactobacillus plantarum CAM 4: Characterization and in vitro evaluation of its antimicrobial efficiency. Journal of Molecular Liquids: 121476.

Luo, X. (2023)**.** Advances in nanomaterial-based electrochemical (bio-) sensors. Microchimica Acta, 190(1): 9.

Nagar, N. and Devra, V. (2019)**.** A kinetic study on the degradation and biodegradability of silver nanoparticles catalyzed Methyl Orange and textile effluents. Heliyon, 5(3): e01356.

Naghmouchi, S.; Al-Zaban, M.I.; Al-Zaben, M.; Alharbi, N. and Bahatheq, A. (2022)**.** Generation and Characterization of Silver Nanoparticles in Mentha pulegium Extract and Evaluation of Biological Activities of the Prepared Extract. Journal of Nanomaterials, 2022.

Nguyen, T.T.T.; Le, H.H.; Truong, T.V.; Doan, T.P.T.; Nguyen, T.T.T. and Nguyen, T.M.L. (2020)**.** Application of the Response Surface Methodology for Green synthesis of silver nanoparticles using a plant extract of shallot. Egyptian Journal of Chemistry, 63(11): 4579-4588.

Palaniyandi, T.; Baskar, G.; V, B.; Viswanathan, S.; Abdul Wahab, M.R.; Govindaraj, M.K.; Sivaji, A.; Rajendran, B.K. and Kaliamoorthy, S. (2023)**.** Biosynthesis of iron nanoparticles using brown algae Spatoglossum asperum and its antioxidant and anticancer activities through in vitro and in silico studies. Particulate Science and Technology: 1-14.

Paramelle, D.; Sadovoy, A.; Gorelik, S.; Free, P.; Hobley, J. and Fernig, D.G. (2014)**.** A rapid method to estimate the concentration of citrate capped silver nanoparticles from UV-visible light spectra. Analyst, 139(19): 4855-4861.

Patil, R.S.; Kokate, M.R.; Jambhale, C.L.; Pawar, S.M.; Han, S.H. and Kolekar, S.S. (2012)**.** One-pot synthesis of PVA-capped silver nanoparticles their characterization and biomedical application. Advances in natural sciences: nanoscience and nanotechnology, 3(1): 015013.

Paulraj, P.; Umar, A.; Rajendran, K.; Manikandan, A.; Kumar, R.; Manikandan, E.; Pandian, K.; Mahnashi, M.H.; Alsaiari, M.A. and Ibrahim, A.A. (2020)**.** Solid-state synthesis of Ag-doped PANI nanocomposites for their end-use as an electrochemical sensor for hydrogen peroxide and dopamine. Electrochimica Acta, 363: 137158.

Ramya, M. and Subapriya, M.S. (2012)**.** Green synthesis of silver nanoparticles. Int J Pharm Med Biol Sci, 1(1): 54-61.

Rane, A.V.; Kanny, K.; Abitha, V. and Thomas, S. (2018). Methods for synthesis of nanoparticles and fabrication of nanocomposites. In *Synthesis of inorganic nanomaterials* (pp. 121-139). Elsevier.

Rezazadeh, N.H.; Buazar, F. and Matroodi, S. (2020)**.** Synergistic effects of combinatorial chitosan and polyphenol biomolecules on enhanced antibacterial activity of biofunctionalized silver nanoparticles. Scientific reports, 10(1): 1-13.

Shantkriti, S.; Pradeep, M.; Unish, K.; Das, V.; Nidhin, S.; Gugan, K. and Murugan, A. (2023)**.** Bioynthesis of silver nanoparticles using Dunaliella salina and its antibacterial applications. Applied Surface Science Advances, 13: 100377.

Sharma, A.; Sharma, S.; Sharma, K.; Chetri, S.P.; Vashishtha, A.; Singh, P.; Kumar, R.; Rathi, B. and Agrawal, V. (2016)**.** Algae as crucial organisms in advancing nanotechnology: a systematic review. Journal of Applied Phycology, 28(3): 1759-1774.

Singaravelan, R. and Bangaru Sudarsan Alwar, S. (2015)**.** Electrochemical synthesis, characterisation and phytogenic properties of silver nanoparticles. Applied Nanoscience, 5: 983-991.

Singaravelu, G.; Arockiamary, J.; Kumar, V.G. and Govindaraju, K. (2007)**.** A novel extracellular synthesis of monodisperse gold nanoparticles using marine alga, Sargassum wightii Greville. Colloids and surfaces B: Biointerfaces, 57(1): 97-101.

Soliman, M.K.; Salem, S.S.; Abu-Elghait, M. and Azab, M.S. (2023)**.** Biosynthesis of silver and gold nanoparticles and their efficacy towards antibacterial, antibiofilm, cytotoxicity, and antioxidant activities. Applied Biochemistry and Biotechnology, 195(2): 1158-1183.

Somasundaram, C.K.; Atchudan, R.; Edison, T.N.J.I.; Perumal, S.; Vinodh, R.; Sundramoorthy, A.K.; Babu, R.S.; Alagan, M. and Lee, Y.R. (2021)**.** Sustainable synthesis of silver nanoparticles using marine algae for catalytic degradation of methylene blue. Catalysts, 11(11): 1377.

Thakkar, K.N.; Mhatre, S.S. and Parikh, R.Y. (2010)**.** Biological synthesis of metallic nanoparticles. Nanomedicine: Nanotechnology, Biology and Medicine, 6(2): 257-262.

Unnisa, A.; Greig, N.H. and Kamal, M.A. (2023)**.** Nanotechnology: A Promising Targeted Drug Delivery System for Brain Tumours and Alzheimer's Disease. Current Medicinal Chemistry, 30(3): 255-270.

Yaqoob, A.A.; Ahmad, H.; Parveen, T.; Ahmad, A.; Oves, M.; Ismail, I.M.; Qari, H.A.; Umar, K. and Mohamad Ibrahim, M.N. (2020a)**.** Recent advances in metal decorated nanomaterials and their various biological applications: A review. Frontiers in Chemistry, 8: 341.

Yaqoob, A.A.; Parveen, T.; Umar, K. and Mohamad Ibrahim, M.N. (2020b)**.** Role of nanomaterials in the treatment of wastewater: A review. Water, 12(2): 495.

Zahran, M.K. and Mohammed, H.A. (2021)**.** Green synthesis of silver nanoparticles using polysaccharide extracted from Laurencia obtuse algae. Egypt J Appl Sci, 36(1): 9-16.